



Research article

The load-bearing of composite slabs with steel deck under natural fires

Marcílio M. A. Filho¹, Paulo A. G. Piloto^{2,*} and Carlos Balsa³

¹ ISISE, Department of Civil Engineering, Universidade do Minho, Campus Azurém, 4800-058, Portugal

² LAETA INEGI, Instituto Politécnico de Bragança, Campus Santa Apolónia, 5300-253, Portugal

³ Research Centre in Digitalization and Intelligent Robotics (CeDRI), Instituto Politécnico de Bragança, Campus Santa Apolónia, 5300-253, Portugal

* **Correspondence:** Email: ppiloto@ipb.pt; Tel: +351-273-303-157;
Fax: +351-273-313-051.

Abstract: Composite slabs with steel deck combine the load-bearing resistance of the steel deck and rebar with the compressive resistance of the concrete (components). Unprotected composite slabs may be exposed to natural fire conditions from below, and steel reduces its load-bearing capacity during the heating stage. In short fire events, with limited deformations, the composite slabs can recover the load-bearing capacity during the cooling stage. This research presents the validation of the numerical model and the development of a parametric study, to evaluate the load-bearing capacity during the fire event. This method includes a time step procedure, based on the average temperature calculation for each component, including the reduction coefficients applied to the design strength of each material. A new proposal is also presented to evaluate the residual load-bearing capacity. In some circumstances, the residual load-bearing can be reduced by more than 20%. The results showed that the highest variation in the load-bearing resistance of composite slabs occurs when the steel temperatures are between 20 and 600 °C, after this temperature, the steel has already lost most of its mechanical strength. Moreover, it was observed that different heating rates and different cooling rates influence the rate of the reduction and recovery of the load-bearing capacity. It was also noticed that the lowest load-bearing capacity of the composite slabs was reached after the end of the heating phase, showing that the stability of the element during the heating phase does not guarantee fire safety during the cooling phase.

Keywords: composite slabs; steel deck; natural fire; load-bearing; residual resistance

1. Introduction

The advantages of using composite slabs in high-rise buildings are mainly associated with the use of the collaborating steel deck, which also acts as permanent formwork, with elevated bending moment resistance, and with the possibility to use with large spans. As mentioned by Jiang et al. [1] the existence of the steel deck reduces the construction time of the composite slabs, as well as reduces the self-weight of the structural element, in comparison to the traditional concrete slab, for the same load-bearing resistance. The composite slab typically has welded wire mesh, working for hogging moments, and usually contains rebars within the ribs, working for sagging moments.

One disadvantage of using composite slabs with unprotected steel deck is related to the possibility of the steel deck being directly submitted to a fire event. The steel deck reduces its strength and stiffness when exposed to elevated temperatures [2]. Neves et al. [3] investigated the residual strength of structural steel cooled after being subjected to high temperatures, finding that for temperatures above 600 °C, the material properties suffered considerable changes in its residual strength. Additionally, fire also reduces the strength of concrete, due to the disintegration of cement's hydration products and bond breaking in the microstructure of the cement paste, which reduces the modulus of elasticity from the concrete, and the extent of this reduction depends on moisture loss, temperature, and type of aggregate [4]. Chang et al. [5] mention that concrete suffers a severe loss of strength after reaching temperatures above 400 °C, due to the dehydration effects of calcium silicate hydrate. Gillie et al. [6] emphasize that one of the main objectives in fire safety engineering is to prevent structures from catastrophic collapse when subjected to fire. Thus, since the composite slabs perform a fundamental role in the stability of the structure during a fire, it is necessary to understand the behavior of the load-bearing capacity (R) of this element under fire.

Li et al. [7] and Filho [8] highlight the importance of evaluating the load-bearing capacity during the cooling phase, as the temperatures in the reinforcement and the unexposed surface of the slab continue to increase during this phase, which indicates the possibility of failure of the structure after the peak temperature of the gas. Seeking to assess the viability of further use of the building after the fire, Nguyen et al. [9] developed experimental tests on composite slabs with a flat steel deck and found that the integrity of the composite slab can be maintained even after four hours of the standard fire, eliminating concrete spalling and minimizing post-fire structural damage. The authors also reported the debonding of the steel deck in certain regions and the steel degradation. The embedded vertical webs and top flanges of the flat decking sustained much lower temperatures compared to that the bottom flanges, helping their contribution to the load-bearing capacity. Molken et al. [10] mentioned that further use of the building after fire may be possible, however, since in most cases the elements do not collapse during fire exposure, but may suffer a permanent loss of their strength, it is necessary to evaluate the residual load-bearing capacity of the structures after a fire, to make decisions about continued use and the need for structural reinforcement.

The fire resistance may be determined according to three criteria, namely the load-bearing (R), integrity (E), and insulation (I). According to EN 1363-1 [11], the fire resistance by insulation criterion (I) is expressed in minutes and refers to the shortest time to reach the average or the maximum temperature on the unexposed surface of the slab, when it increases 140 °C or 180 °C above the initial average temperature, respectively. The integrity criterion is usually satisfied due to the existence of the steel deck, avoiding the passage of flames and hot gases through the slab. The load-bearing criterion considers the maximum deflection and the rate of deflection, imposing some

limits. Beyond this, annex D of Eurocode 4 Part 1-2 [12] presents simplified methods that can be used to find the load-bearing resistance under standard fire. This investigation fills a gap on the fire resistance of composite slabs under natural fire, using a time step thermal procedure, allowing the calculation of the sagging moment (load-bearing resistance under natural fire).

It is worth mentioning that most designers rely on the recommendations and parameters of EN1994-1-2 [12] to evaluate the behaviour of concrete and steel composite structures submitted to fire. However, the design criteria for composite slabs subjected to fire have not been revised for decades [13]. For example, Bolina et al. [14] concluded that the simplified methods proposed by EN1994-1-2 present good convergence for the temperatures in steel deck, but the same was not observed for the temperatures in concrete and rebar. This highlights the benefits of using calibrated numerical models and the need to investigate and improve the simplified methods to determine the temperature distribution in composite slabs since temperatures are fundamental for the analysis of fire exposure structures [15].

Thus, given that the standard assumes that the fire resistance criterion (R) is satisfied when the load-bearing function is maintained during the required time of fire exposure, this investigation used a non-linear thermal analysis (ANSYS and MATLAB) to determine the load-bearing capacity of composite slabs when subjected to natural fire, including the heating and cooling phases. This procedure will prevent the collapse of the composite slab, based on the simplified method, only available to the standard fire by the annex D in Eurocode 4 Part 1-2 [12], and also seek the residual strength of the structure for possible reuse. A preliminary and simplified approach is also presented to estimate and evaluate the bending resistance of the composite slabs during and after a natural fire, shedding light to researchers on possible ways to consider the cooling phase on the simplified method and to evaluate, in a simplified way, the residual strength of the elements. The numerical models were validated through experimental results presented by other authors [16,17], and a parametric study was carried out considering different steel deck profiles, different natural fire scenarios, and different concrete cover thicknesses.

2. Materials and methods

To determine the load-bearing capacity of the composite slabs, the advanced calculation method was used following the recommendations of the Eurocode EN1994-1-2 [12]. The advanced method is based on three-dimensional finite element models. The parametric study included a total of 128 thermal simulations, 64 of which were performed using ANSYS and the remaining 64 simulations using MATLAB. Moreover, thermal simulations for validation of the numerical models were performed using experimental data presented by other authors [16,17].

2.1. Load-bearing capacity

The fire rating (R) applied to the composite slabs with steel deck is defined in Europe by the time to support the test load [18]. The time is set in complete minutes and may change from 15 to 240 min. The experimental test of composite slabs should be developed in horizontal furnaces and tested under EN 1365-2 [19] and EN1363-1 [11], with fire applied from below only.

The Eurocode EN1994-1-2 [12] also presents an alternative method to define the load-bearing capacity of the composite slabs with steel deck, using the simplified method. The main focus of the

design method is on providing equations to determine the temperature of the components. These equations were derived by Both [20], who made an approximation after several numerical simulations. Although not mentioned in EN1994-1-2, the average moisture content of the concrete was considered equal to 4% for Normal Weighted Concrete (NWC) and 5% for Light Weight Concrete (LWC). It is also assumed that the deck will be perfectly bonded to the concrete, which is not the case verified in several experimental tests and other numerical models developed by Piloto et al. [21–24].

The sagging moment may be determined for standard fire only, using trapezoidal and re-entrant steel deck profiles, dividing the bending resistance into four components affected by the temperature (lower flange, web, upper flange, rebar) and one component which is not affected by the temperature (concrete under compression). The affected components will have their design strength reduced by the temperature effect. The temperature depends on the geometry and thermal properties of the materials and is determined by empirical coefficients, according to annex D of EN1994-1-2.

Figure 1 represents the cross-section of a trapezoidal composite slab and the stress field used for the calculation of the sagging moment. After the average temperature calculation in the steel components responsible for tensile stresses, one can determine the reduction in the yield strength, according to the temperature level. Once the stresses are obtained, the sum of the tensile forces from the steel and the compressive forces from the concrete component should be in equilibrium, see Eq 1. This equation determines the plastic neutral axis (x_{pl}) of the composite slabs.

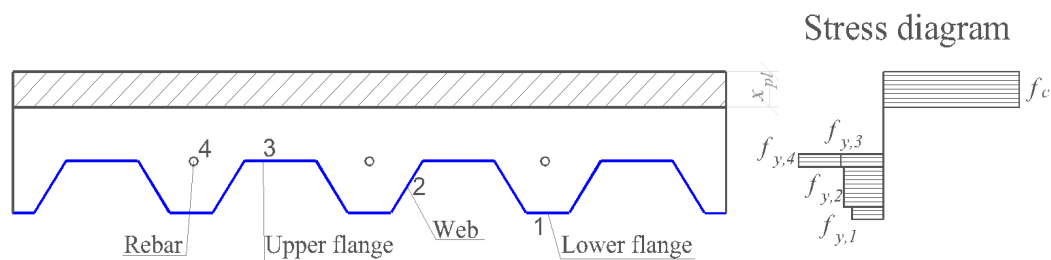


Figure 1. Stress diagram in composite slabs for the calculation of the sagging moment.

$$\sum_{i=1}^n A_i k_{y,\theta,i} \left(\frac{f_{y,i}}{\gamma_{M,fi,a}} \right) + \alpha_{slab} \sum_{j=1}^m A_j k_{c,\theta,j} \left(\frac{f_{c,j}}{\gamma_{M,fi,c}} \right) = 0 \quad (1)$$

Where α_{slab} is a reduction coefficient equal to 0.85 for composite slabs; $f_{y,i}$ is the yield stress associated to the steel component of area A_i , so that it must be considered negative if it is in the compressed region, and positive if it is in the tensioned region; $f_{c,j}$ is the concrete strength at 20 °C referring to the area A_j present above the neutral axis and responsible to resist compression.

In order to guarantee a good prediction of the mechanical model for the composite slabs, it is required to have a good prediction of the temperature distribution in the composite slabs. Jiang et al. [25] also warn for the need for a better understanding of the thermal behaviour of composite slabs, as the thermal profiles depend on the heat transfer boundary conditions, concrete moisture content, thermal properties of the concrete, and rib geometry.

Considering that the temperature in the compressed region of the concrete is not uniform, and the problems involved in obtaining a good prediction of the temperature profile in the region, a

simplification will be adopted by taking $k_{c,\theta,j}$ as 1 during the evaluation of the load-bearing capacity under fire, considering that the compressed concrete will not suffer considerable strength reduction. However, for the residual load-bearing capacity assessment, after the fire event, a different approach will be adopted and detailed in section 3.3.

After finding the neutral axis position, the sagging moment of the composite slabs may be determined. The design moment resistant $M_{f,i,t,Rd}$ (positive) may be determined using Eq 2.

$$M_{f,i,t,Rd} = \sum_{i=1}^n A_i z_i k_{y,\theta,i} \left(\frac{f_{y,i}}{\gamma_{M,f,i,a}} \right) + \alpha_{slab} \sum_{j=1}^m A_j z_j k_{c,\theta,j} \left(\frac{f_{c,j}}{\gamma_{M,f,i,c}} \right) \quad (2)$$

To calculate the load-bearing capacity of the composite slabs during a fire, Eqs 1 and 2 were used following the recommendations of EN1994-1-2 [12]. For the calculation of the initial bending resistance (at room temperature), the reduction coefficients $k_{y,\theta,i}$ and $k_{c,\theta,j}$ are both set to 1.

This failure mode is based on the assumption that all the components of the composite slabs are capable of reaching their plastic stresses.

2.2. Numerical model validation

Two different finite element models are presented. The numerical model developed in MATLAB uses linear tetrahedral finite elements with 4 nodes for mesh generation, each node having one degree of freedom (temperature). In ANSYS, three different linear finite elements are used: 3D finite element SOLID 70 with 8 nodes, being used to represent the concrete, shell finite element SHELL131, with 4 nodes, being used to represent the air-gap layer and the steel deck, since this element is ideal to model thin-walled structures; unidimensional finite element LINK33, with 2 nodes is being used to represent the rebars and the steel mesh.

The boundary conditions used to simulate the exposed surface and the unexposed surface are following the recommendations of the Eurocode EN1991-1-2 [26]. For the thermal analysis, a heat flux by convection and radiation is considered on the exposed surface of the composite slab. Therefore, for natural fire events, the coefficients are defined in Figure 2.

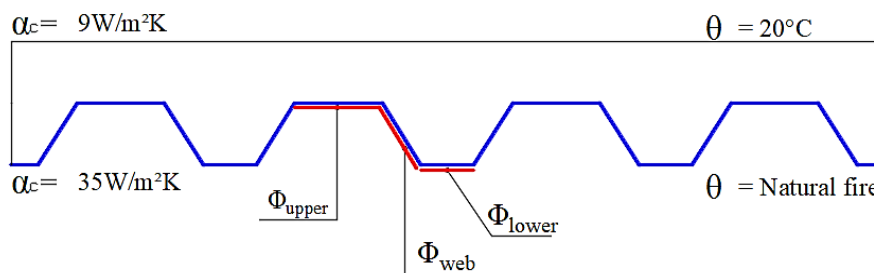


Figure 2. Boundary conditions for the composite slabs exposed to natural fire.

The thermal properties of the materials follow the recommendation of the Eurocode EN1993-1-2 [27] for the steel and EN1994-1-2 [12] for the concrete. An air layer is considered between the steel deck and the concrete, with a thickness of 0.5 mm, as suggested by Piloto et al. [23,24]. This effect has been included due to the debonding effect, due to the existence of different thermal expansion coefficients between both materials (steel and concrete). This debonding

effect is identified by the name “air-gap”. Therefore, in order to model this effect, additional thermal properties are required for the air model [28].

This model considers different view factors for the steel deck components (Φ_{upper} , Φ_{web} , and Φ_{lower}) of both trapezoidal and reentrant steel profiles. This model differs from the current version of the EN1994-1-2 [12], affecting the heat transfer by radiation. The cross string method developed in 1950 by HC Hottel is used to calculate the view factors in the web (Φ_{web}) and the upper flange (Φ_{upper}). The view factor for the lower flange (Φ_{lower}) is equal to 1.

Both numerical models developed in ANSYS and MATLAB have been validated, using finite element models from natural fire tests, in order to evaluate the reliability and accuracy of the numerical results. The fire tests developed in 2011 by Guo and Bailey [16] were selected. These authors performed tests on seven composite slabs with steel deck, subjected to different natural fire scenarios and different loading levels. The slabs had a steel deck type CF60/1.2, with a thickness of 1.2 mm and yield strength of 378 MPa. The reinforcement mesh used steel type (A193), with bars of 7 mm in diameter, spaced every 200 mm, as indicated in Figure 3.

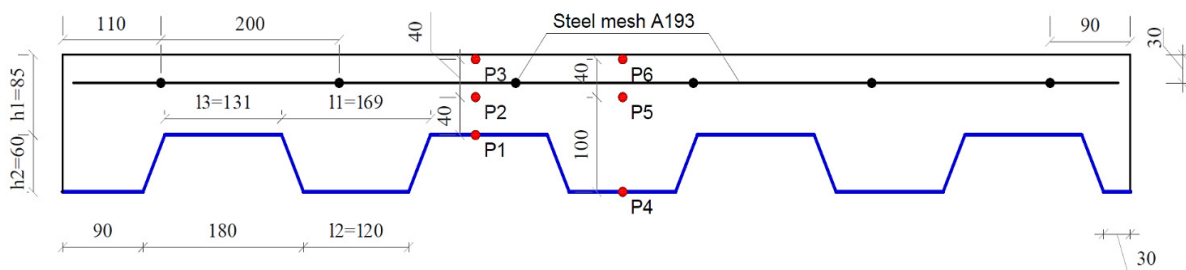


Figure 3. Geometric of the tested composite slabs [16].

For the validation of the models, three of the seven slabs, tested by Guo, Bailey [16], were selected, so that each one was submitted to a different natural fire scenario as indicated in Table 1. Details about the concrete compressive strength, moisture, and failure load are also included.

Table 1. Characteristics of the tested composite slabs used for validation.

Slab N°	Concrete strength (MPa)	Fire scenario	Moisture (%)	Applied load (kN)	Failure load after fire (kN)
Slab 1	36.4	Fire 1	1,50	44	-
Slab 2	37.8	Fire 2	2,00	44	262
Slab 3	21.1	Fire 3	1,86	44	204

The three fire scenarios presented in Table 1, have a heating and a cooling phase. The gas furnace temperatures are depicted in Figure 4. The Fire 1 and Fire 3 scenarios have a 40-minute heating phase, with the same heating rate, but different cooling phases, with the Fire 3 having a slower cooling rate, resulting in a longer fire event. The fire scenario Fire 2, presents a 90-minute heating phase, with a lower maximum temperature than the other fire scenarios, and includes a fast cooling phase.

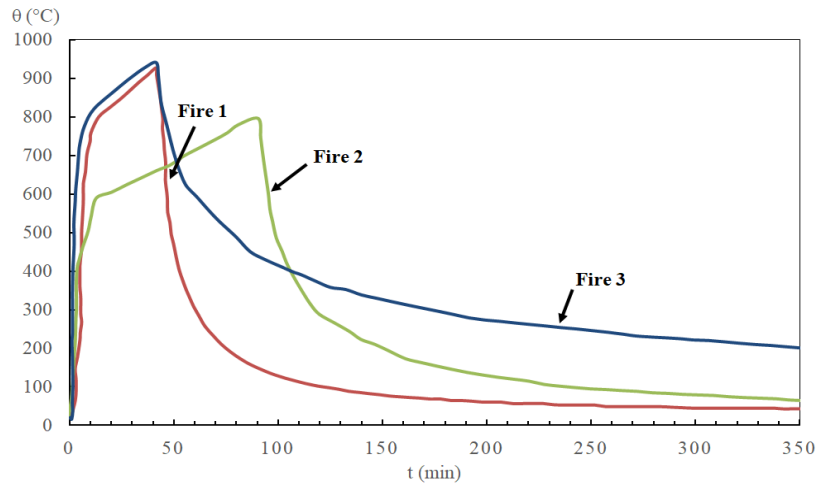


Figure 4. Fire scenarios [16].

2.3. Parametric study

This parametric study includes 64 thermal simulations using ANSYS and 64 thermal simulations using MATLAB, to evaluate the effects of different fire scenarios, the effect of different geometries, and different concrete thicknesses. All the composite slabs are using the same reinforcement, 3 rebars of steel S500 with $\text{Ø}10$ mm diameter, always located at a distance h_2 from the exposed surface. The reinforcement mesh uses an S500 steel grid with $\text{Ø}6$ mm diameter bars, spaced every 150 mm and positioned 20 mm below the unexposed surface of the slab as shown in Figure 5. The conventional concrete class used for the models is type C25/30 with 2% moisture.

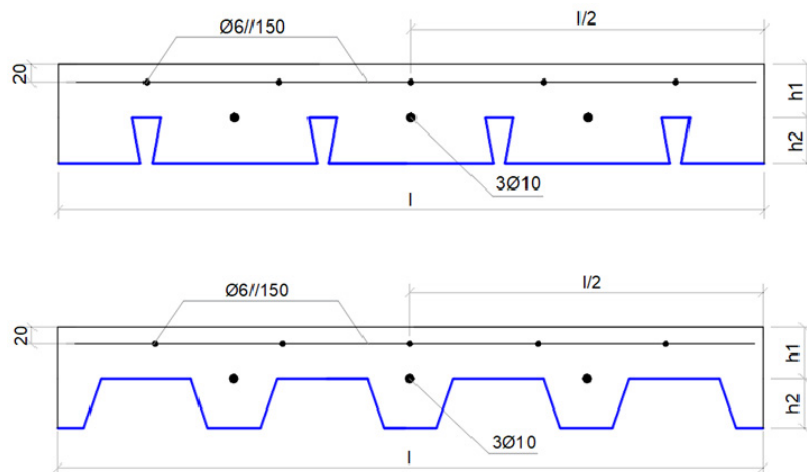


Figure 5. The geometry of the parametric models.

The study considers the load-bearing capacity of a simply supported composite slab, with 4 m length, as shown in Figure 6.

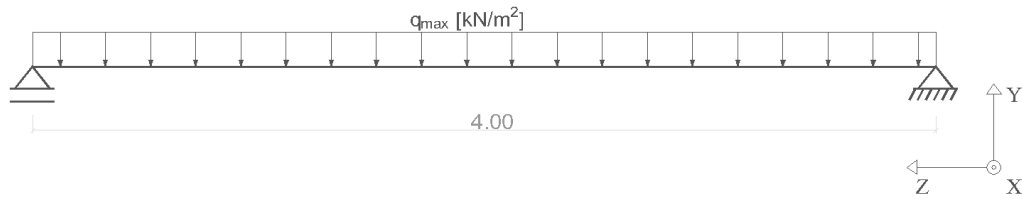


Figure 6. Boundary Conditions to determine the sagging moment resistance.

The parameters were selected to obtain some representativeness of this building element, testing different reentrant and trapezoidal geometries for the steel deck, selecting also different concrete cover thicknesses (h_1). These analyses were developed to find the load-bearing resistance under different types of natural fire scenarios, considering the effect of different heating and cooling rates. Therefore, parametric simulations were performed using four different commercial steel deck profiles (Multideck 50, Bondeck, Polideck 59S, and Confraplus 60, with widths equal to 0.6, 0.8, 0.84, and 0.828 m, respectively), using four different concrete thicknesses above the steel deck ($h_1 = 40, 60, 80$ and 100 mm) and four different natural fire curves (Parametric i). Three fire curves show a similar heating rate to the standard fire ISO 834 [29], and another curve with a higher heating rate, see Figure 7 and Table 2.

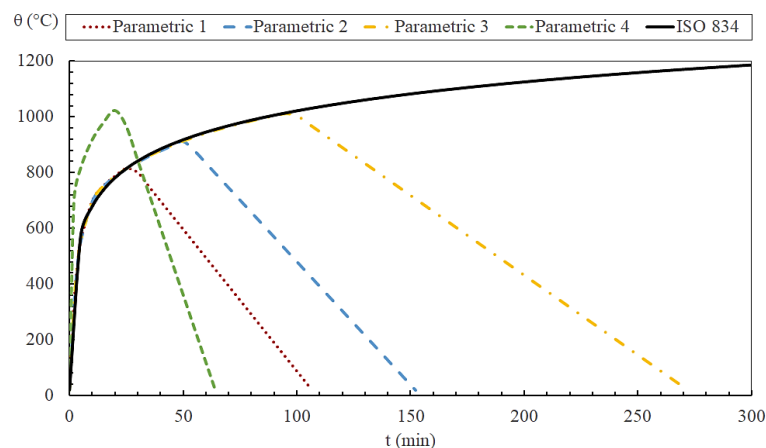


Figure 7. Parametric fire curves.

Table 2. Characteristics of the tested composite slabs used for validation.

Fire scenario	Maximum temperature (°C)	Time at maximum temperature (min)	Fire duration (min)
Parametric 1	825.79	27.43	106
Parametric 2	915.38	50.93	152
Parametric 3	1010.46	95	272
Parametric 4	1036.60	22	64

Using the numerical results obtained in the thermal analysis with ANSYS, the temperature of the steel components has been averaged, throughout the fire duration, helping to determine the neutral plastic axis and the sagging moment of the slab throughout the heating and cooling phases.

3. Results and discussion

The results obtained from the validation of the numerical models and the parametric study will be discussed and presented below.

3.1. Numerical model validation results

The results obtained for the validation of the model used for the composite slab 1 and 3 are shown in Figure 8, which shows the comparison between the temperatures obtained in the experimental tests and the numerical models, using the ANSYS and MATLAB. The points where the temperature curves are collected are represented in Figure 3. The results for Slab 1 show good convergence. The results for slab 3, on the other hand, show a higher discrepancy in concrete temperatures during the cooling phase, which has a small cooling rate and perhaps should have used different convection coefficients in the unexposed surface.

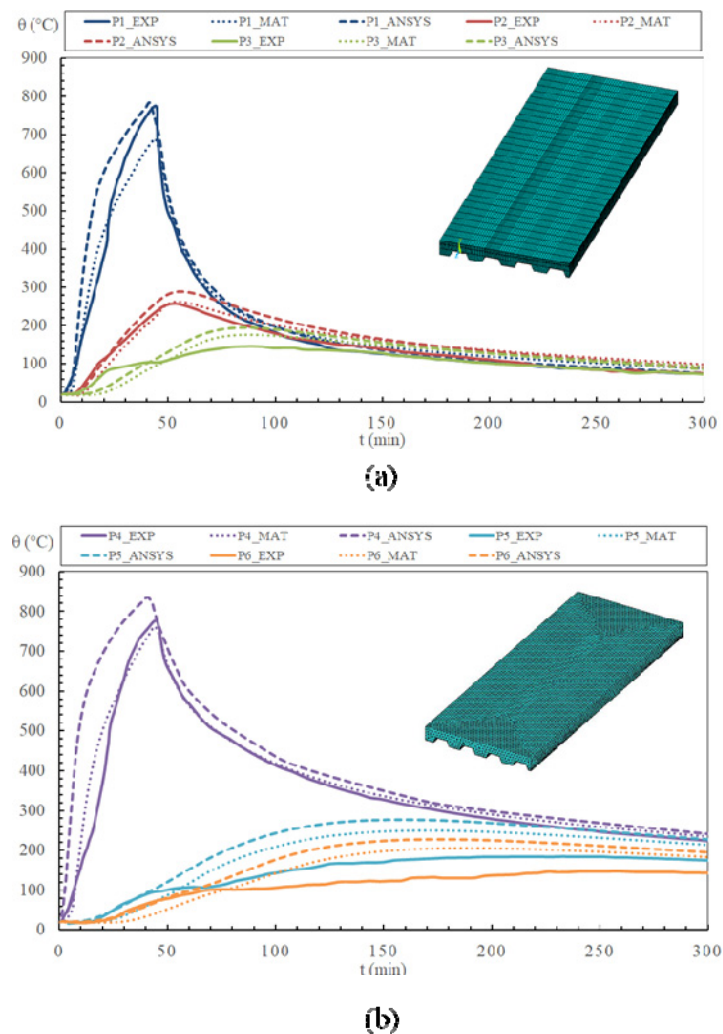


Figure 8. Numerical model validation using MATLAB and ANSYS. (a) Composite slab 1, (b) Composite slab 3.

The results obtained with the numerical model of MATLAB present a better approximation of the experimental results during the cooling phase, mainly in the region of the steel deck, as can be observed in the curves of points P1 and P4. At point P2 and P5, a good agreement with ANSYS numerical model is observed during the heating phase, whereas for points P3 and P6, which are located 5 mm from the unexposed surface, it is possible to observe a small difference at the beginning of the fire. In general, the temperatures obtained in the numerical model, observed in the concrete during the cooling phase, end up slightly overestimating the measured temperatures. This behaviour is even higher for the model results presented in Slab 3, which represents a long cooling phase with a smaller cooling rate in the furnace temperature. The difference between ANSYS and MATLAB predictions can be attributed to the model used for the “air-gap” layer. This MATLAB model is represented by solid finite elements, whereas in ANSYS the model is represented by two overlapping shell elements with coincident nodes (the air gap is superposed to the steel deck).

After performing the thermal simulations, the temperatures in every steel component are collected during the fire event, in order to determine the evolution of the load-bearing capacity of the composite slabs. Figure 9 presents the test setup, as well as the boundary conditions adopted in the study. It should be noted that the load (P) shown in Table 1 was applied through the hydraulic jack, the self-weight of the slabs was 9.6 kN, and the weight of the plates and the loading system was 8.18 kN.

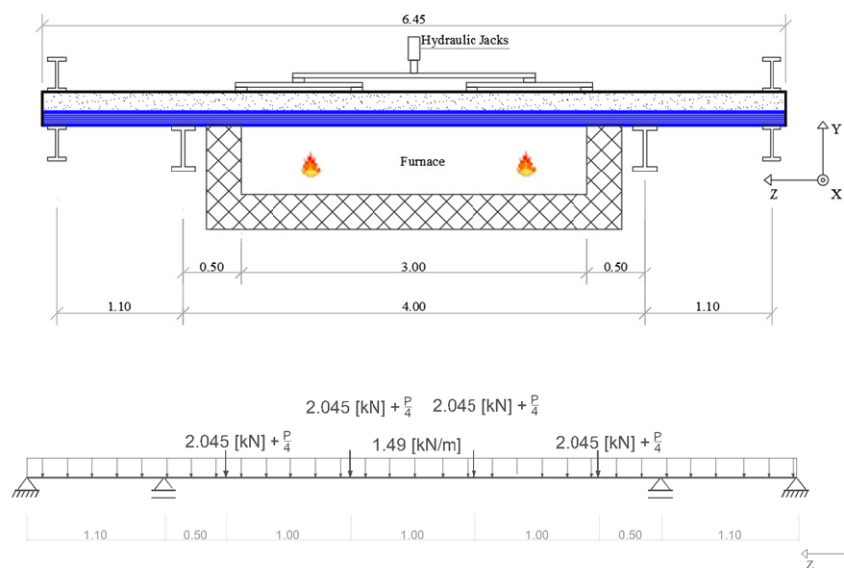


Figure 9. Location of the supports, load application points, and the furnace in the composite slabs tested [16].

Figure 10 shows the behaviour of the plastic neutral axis position and the load-bearing during the fire event. It should be noted that the vertical dotted lines represent the time when the gas reaches maximum temperature. These results are determined by using Eqs 1 and 2. The yield strength reduction coefficients of the steel components ($k_{y,\theta}$) are determined by linear interpolation using the tabulated values provided in standards EN1993-1-2 [27] and EN1994-1-2 [12], for the heating and cooling phases respectively, and considers the complete reversibility of the material. Moreover, due to the low conductivity of the concrete, a large temperature gradient is expected, and no calculation

procedure is currently proposed in EN1994-1-2 for the calculation of the concrete temperature to determine the sagging moment.

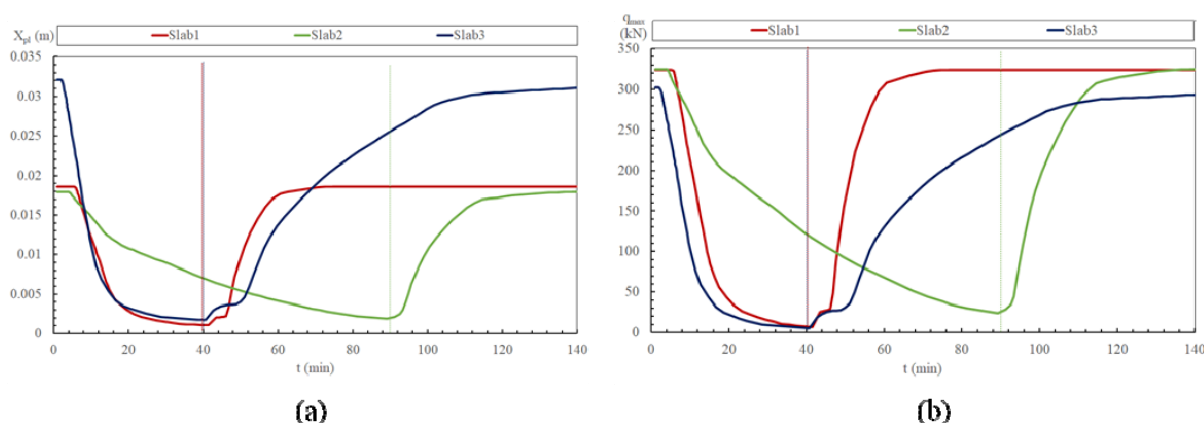


Figure 10. Load-bearing capacity of the three composite slabs. (a) Plastic neutral axis during fire, (b) Load-bearing resistance during a fire.

It is possible to observe from Figure 10, that the load-bearing capacity of the composite slabs with steel deck tested by Guo and Bailey [16], behave similarly concerning the neutral axis position, being the load-bearing capacity reduced during heating, and recovered during cooling. It can be seen that the rate of bending resistance recovery during cooling is higher than the rate of bending resistance loss during heating. This occurs because it is considered that the phase of the fire influences the behaviour of the mechanical properties of the steel. Moreover, it is possible to notice in the loss of the load-bearing capacity of the Slab 2 is developed at a lower rate. This may be justified by the existence of two heating rates, being the rate of the second heating phase lower than the first, see Figure 4. The recovery of the load-bearing capacity of Slab 3 takes more time in comparison to the recovery of Slab 1. This happens because Slab 1 has the highest cooling rate.

It should also be noted that this study was conducted based on the assumption of the reversibility of the strength capacity of steel and concrete. However, due to the high thermal sensitivity of steel, complete reversibility is not generally observed, as mentioned by Tao et al. [30]. According to these authors, few effects are expected for heating below 500 °C, however, when steel is exposed above 500 °C, the reduction in steel strength is notable, due to the removal of the residual stresses. This observation is in agreement with previous experimental tests developed by Piloto et al. [31], which also demonstrated that the residual yield strength depends on the cooling rate.

According to the experimental results, see Table 1, the load at failure for Slab 2 was 262 kN. This load level is reached during the cooling phase at around 106 min, see Figure 10. At this time the gas temperature is still around 450 °C. This indicates that the reversibility of the load-bearing capacity of the slabs during the cooling phase does not occur constantly and totally, and highlights that the final strength of the slabs after the fire is lower than the initial strength. Figure 11 presents the temperature of the cross-section of Slab 2 obtained in ANSYS, at the time when the slab reaches the load of 262 kN.

Figure 11 shows that the unexposed surface of the concrete has some regions at 112.4 °C and some other regions with temperatures of 222.4 °C. This non-uniform behaviour of the temperature

distribution in this region of the concrete highlights the difficulty to determine the reduction of the compressive strength of the material, consequently impacting the prediction of the bending resistance of the slab concerning the sagging moment.

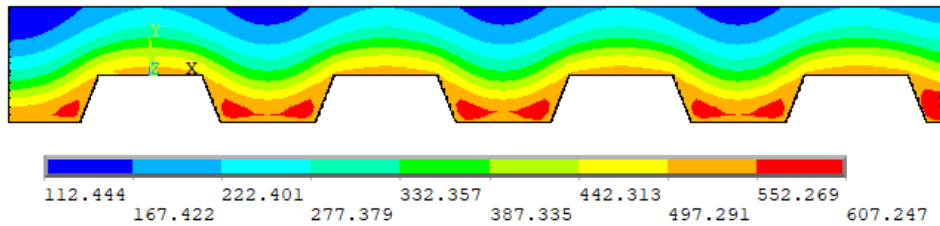


Figure 11. The temperature profile of Slab 2 at 106 min.

3.2. Load-bearing capacity during fire of parametric models

As mentioned by Filho [8] the thickness of the concrete slab over the steel deck, h_1 , influences the temperature of the steel components, thus, the position of the neutral axis varies for the steel profiles with different thicknesses h_1 for the same time or fire rating time. Thus, the position of the neutral axis, measured from the unexposed surface, has a slight difference according to the thickness of the concrete, due to the difference in temperatures of the steel components. Figure 12 presents the behavior of the plastic neutral axis position, using a concrete thickness $h_1 = 100$ mm when all composite slabs are submitted to the Parametric 1 fire, and the load-bearing resistance for the case of a Polideck 59S steel deck.

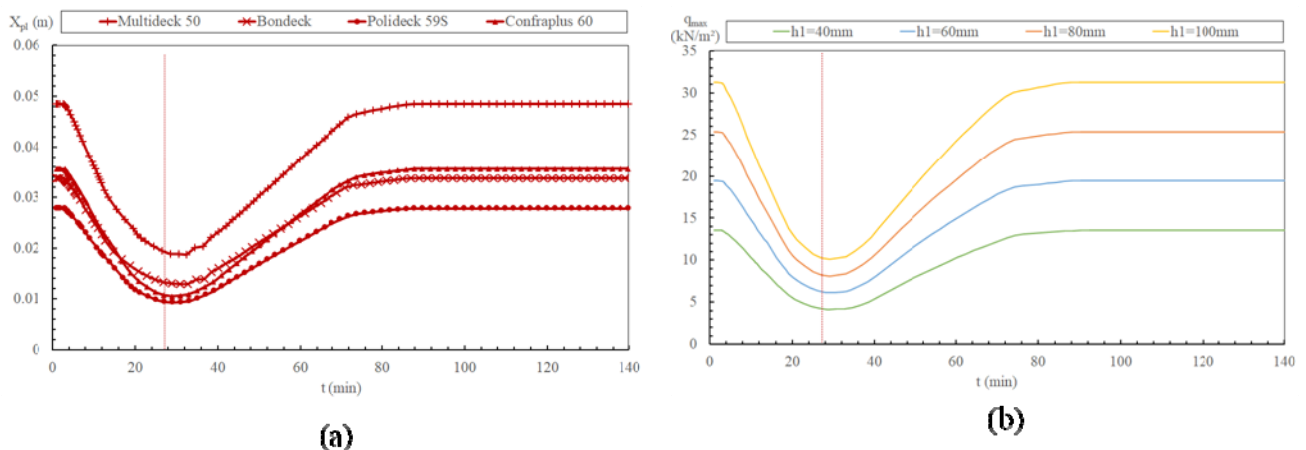


Figure 12. Load-bearing capacity of the composite slabs under Parametric 1 fire scenario. (a) Plastic neutral axis position during the Parametric 1 fire for $h_1 = 100$ mm; (b) Load-bearing resistance of Polideck 59S composite slabs.

It is worth mentioning, that all the profiles, present similar behaviour in the variation of the neutral axis position during the fire. Furthermore, it is observed that the load-bearing capacity follows the behaviour of the neutral axis movement curve during the fire. It is also noted that the rate of load-bearing capacity reduction during the heating period is higher than the rate of the load-

bearing recovery during cooling, which occurs gradually during the cooling period. This is because, although the mechanical strength behaviour of the steel is more favourable during cooling, the cooling rate is lower than the heating rate. It should be noted that all the geometric profiles analysed, presented the same behaviour when submitted to the Parametric 1 fire scenario, changing only the maximum load-bearing resistance.

Figure 13 presents the temperature profiles of the Polideck 59S slabs, at the instant of time when the composite slabs reach the lowest value of load-bearing capacity, when subjected to the Parametric fire scenario 1.

It can be seen in Figure 13 that as the thickness of the concrete layer increases, the temperatures in the unexposed region of the slab tend to become more uniform, and consequently, the concrete in this region has a uniform reduction in its compressive strength.

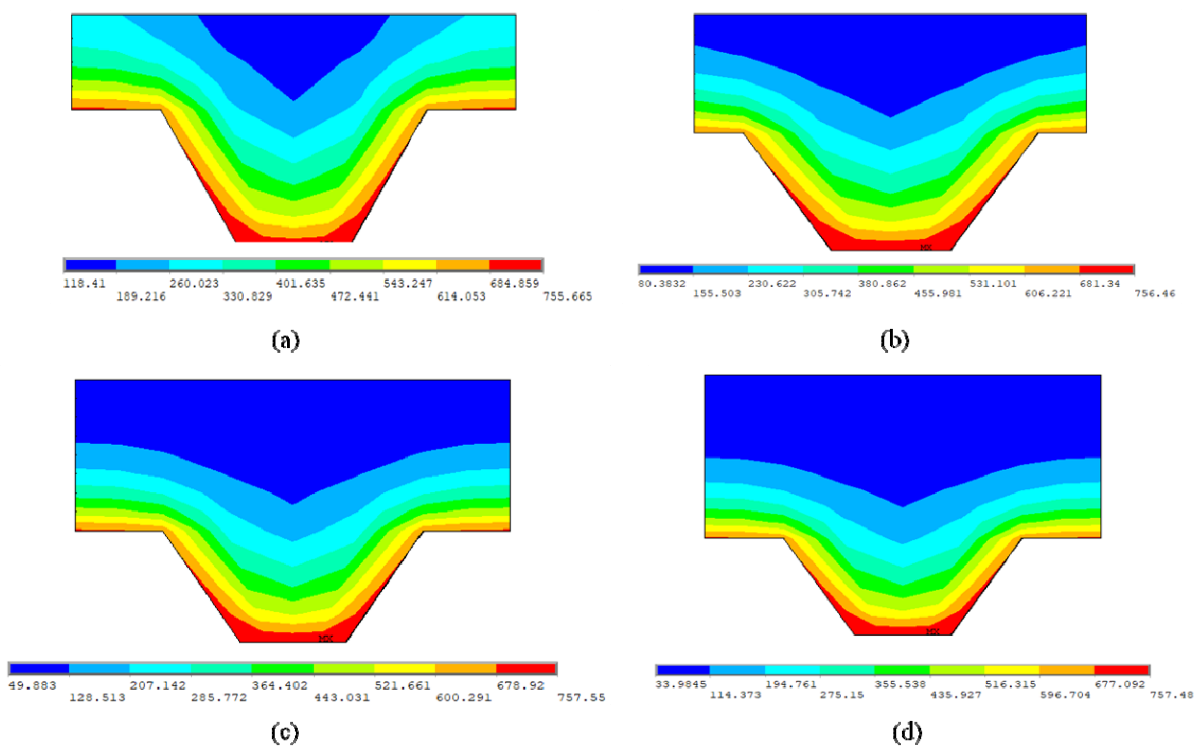


Figure 13. Temperature profile at the instant of lowest value of load-bearing capacity of Polideck 59S slabs for different values of h_1 : (a) $h_1 = 40$ mm; (b) $h_1 = 60$ mm; (c) $h_1 = 80$ mm; (d) $h_1 = 100$ mm.

Figure 14 presents the position of the plastic neutral axis and the load-bearing capacity of the Bondeck slabs along with a Parametric 2 fire scenario.

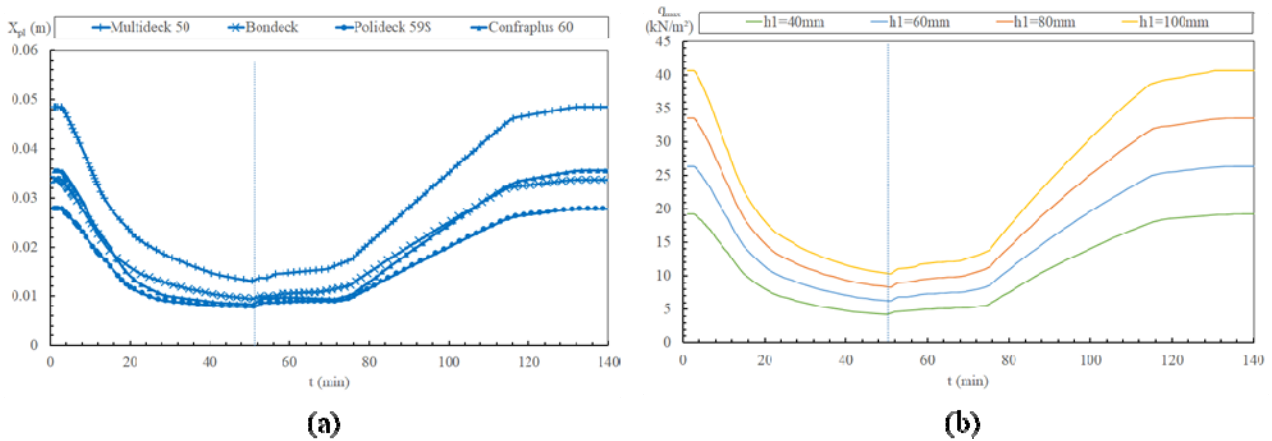


Figure 14. Load-bearing capacity of the composite slabs under Parametric 2 fire scenario. (a) Behaviour of the plastic neutral axis during a fire; (b) Resistant load behaviour of Bondeck slabs during a fire.

It is possible to observe that approximately between 30 and 70 min of fire, there is little change in the bending resistant capacity of the slabs. This stabilization phase occurs during the period in which the temperatures in the steel components are above 600 °C, at this temperature, the steel has already lost most of its strength capacity, having a small variation in temperatures above.

It is important to note that the value used for the emissivity of steel is 0.7, as defined in the standard EN 1993-1-2 [27]. However, Hamerlinck et al. [32] describe that in the case of galvanised steel decks, the emissivity is temperature-dependent due to the existence of the zinc layer. According to the author, until reaching the temperature of 400 °C, the emissivity of galvanised steel is lower than that of concrete. However, with increasing temperature, there is an increase in the emissivity value of the steel deck due to the darkening of the surface resulting from the melting of the zinc layer.

Figure 15 presents the temperature profiles of the Bondeck slabs, for the time when the slabs reached the lowest load-bearing capacity during the fire. Similar conclusions can be pointed out to the behaviour of the unexposed surface, but for this steel deck geometry, the heat flows less through the upper flange, resulting in a more homogeneous temperature distribution in this region.

Figure 16 represents the behavior of the composite slabs under the Parametric 3 fire. The load-bearing capacity curves of the composite slabs have the same shape variation, as previously presented, however, it's perceptible that for the Parametric 2 fire scenario, there is a slight recovery of the neutral axis position in the initial instants of cooling, since, for the Parametric 3 fire scenario, the neutral axis position remains almost constant. This effect indicates that the longer the heating phase is, the worse are the thermal effects on the load-bearing capacity of the slabs during the initial stages of cooling.

Figure 16, also presents the load-bearing capacity of the Multideck 50 composite slab when submitted to the Parametric 3 fire scenario. It can be seen that the lowest load-bearing capacity value reached by the composite slabs occurs at the beginning of the cooling stage. Gernay and Franssen [33] warn to the fact that the stability exhibited by the structure when reaching the maximum temperature at the end of the heating, does not guarantee that the structure will not collapse during the cooling stage, because usually, the load-bearing capacity of an element keeps decreasing after the end of the

heating. This behaviour is expected because, although the temperatures in the steel deck follow the behaviour of the gas temperature, the highest temperature in the steel rebars occurs during the cooling phase, when the biggest reduction of its yield strength occurs. This effect was also observed by Filho [8], who has identified the “heat bubble” effect during the advanced stage of cooling, which means a concentration of heat is formed in the ribs of the slabs, where the rebars are located.

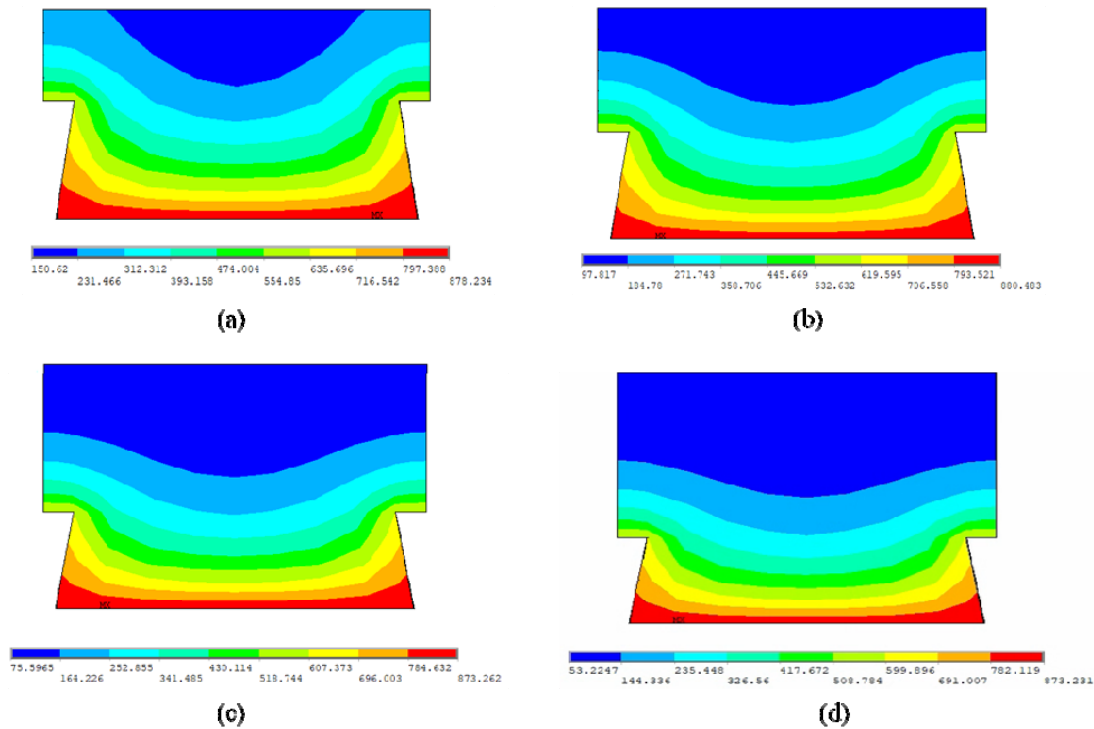


Figure 15. Temperature profile at the instant of the lowest value of the load-bearing capacity of the Bondeck slabs for different values of h_1 : (a) $h_1 = 40$ mm; (b) $h_1 = 60$ mm; (c) $h_1 = 80$ mm; (d) $h_1 = 100$ mm.

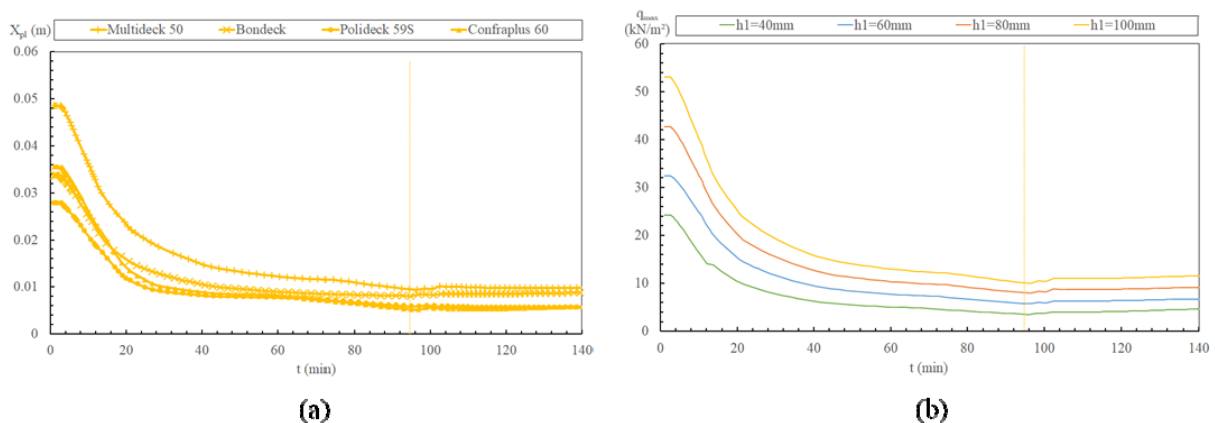


Figure 16. Load-bearing capacity of slabs subjected to the Parametric 3 fire scenario. (a) Behaviour of the plastic neutral axis during a fire; (b) Resistant load behaviour of Multideck 50 slabs during a fire.

The temperature profiles of the Multideck 50 composite slabs are presented in Figure 17 for the time when they reached the lowest value of load-bearing resistance.

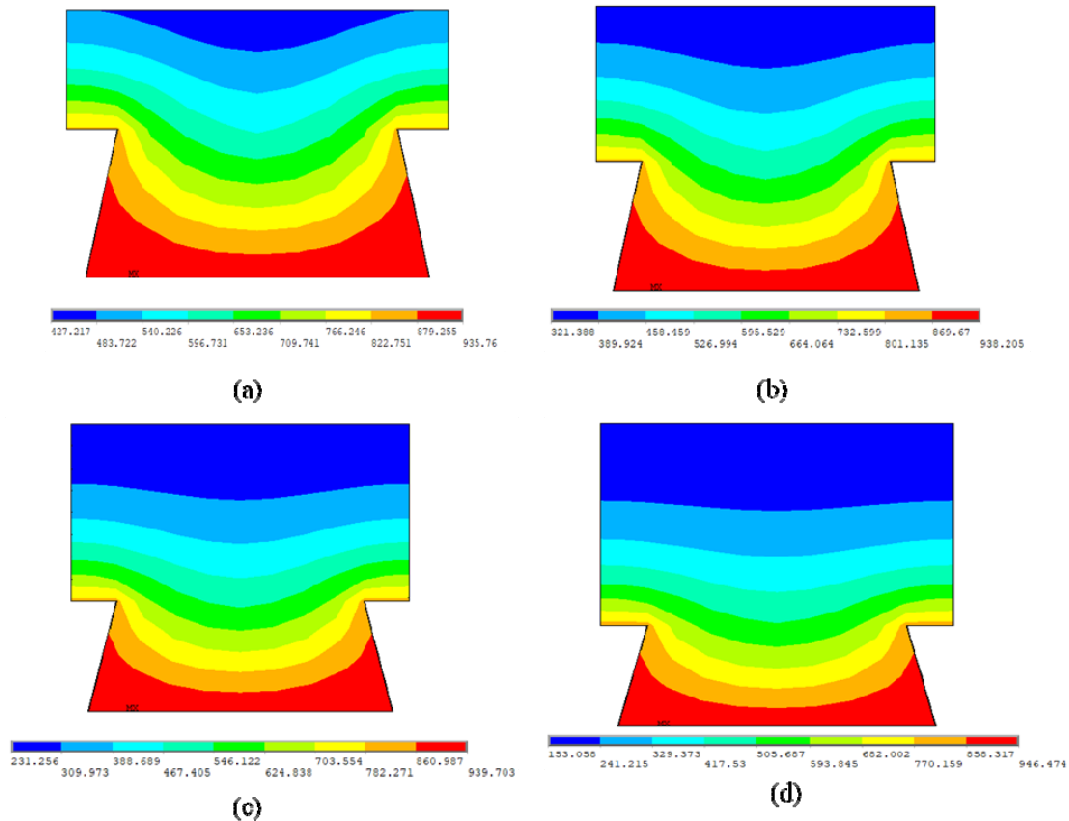


Figure 17. Temperature profile at the instant of the lowest value of load-bearing capacity of Multideck 50 slabs for different values of h_1 : (a) $h_1 = 40$ mm; (b) $h_1 = 60$ mm; (c) $h_1 = 80$ mm; (d) $h_1 = 100$ mm.

Finally, it can be seen in Figure 18, that the profiles subjected to the Parametric 4 fire scenario present an abrupt reduction in load-bearing capacity in the initial stage, due to the high heating rate. Furthermore, it can be seen that the four Confraplus 60 models showed a similar relative load-bearing capacity reduction, with the models reaching the lowest value of approximately 22% of the initial load-bearing capacity. However, it should be noted that the higher the concrete cover thickness h_1 is, the greater the initial load-bearing capacity of the slabs, so the bigger is the initial strength of the slab, the bigger is the total reduction in its load-bearing capacity. For instance, the Confraplus 60 model with $h_1 = 40$ mm thickness suffered a total reduction in its load-bearing capacity of 12.48 kN/m^2 , whereas the model with $h_1 = 100$ mm thickness suffered a reduction of 29.99 kN/m^2 .

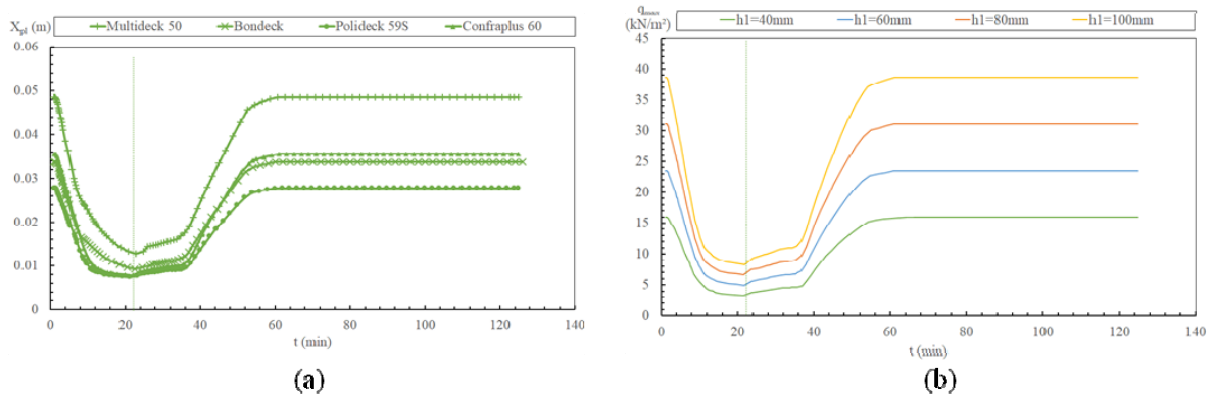


Figure 18. Load-bearing capacity of slabs subjected to the Parametric 4 fire scenario. (a) The position of the plastic neutral axis during a fire; (b) Load resistance behaviour of Confraplus 60 slabs during a fire.

Figure 19 shows the temperature profiles of the Confraplus 60 slabs, for the time when they reached the lowest value of load-bearing capacity. The temperature variation along the profile presented by the slabs submitted to this fire scenario is noteworthy so that the temperatures on the unexposed surface are considerably lower than on the exposed surface. This occurs because this fire scenario presents the highest heating rate, so that the heat flux, which leaves the unexposed surface, is considerably smaller than the incoming heating flux on the surface directly exposed to the fire.

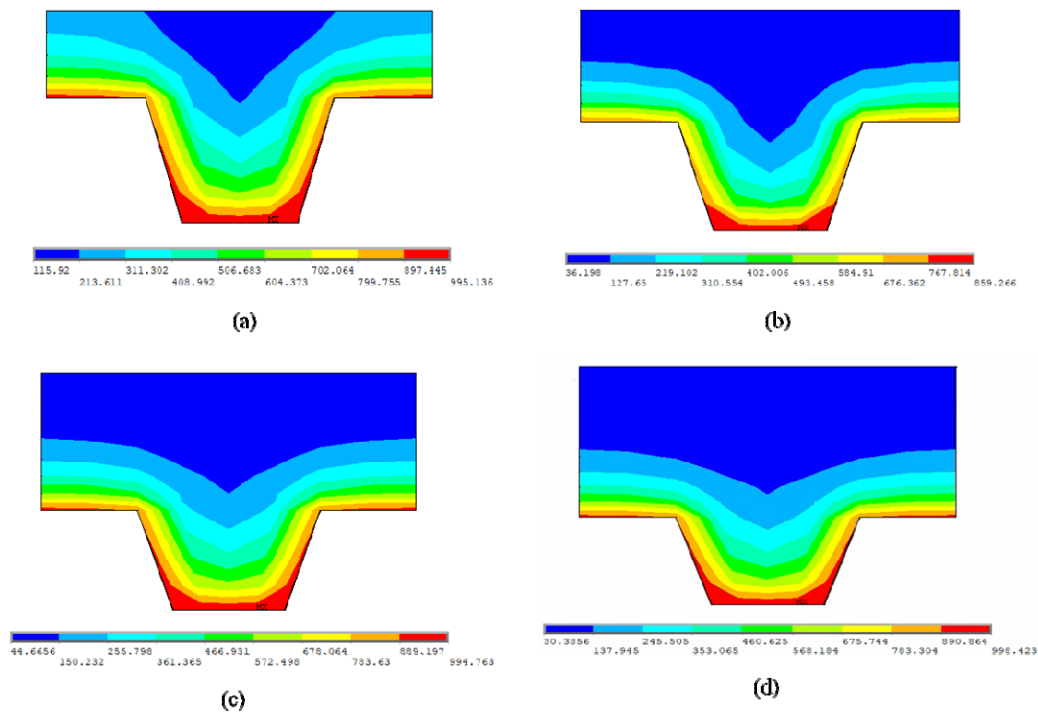


Figure 19. Temperature profile at the instant of the lowest value of the load-bearing capacity of the Confraplus 50 slabs for different values of h_1 : (a) $h_1 = 40$ mm; (b) $h_1 = 60$ mm; (c) $h_1 = 80$ mm; (d) $h_1 = 100$ mm.

3.3. Residual load-bearing capacity of parametric models

Bearing in mind that for models with higher concrete cover thickness, $h_1 = 100$ mm, the temperatures in the unexposed region of the slab are more uniform, a simplified calculation of the residual loadbearing capacity of these models was carried out. The highest average temperature during the fire event, on the unexposed surface of the slab, was used to determine the residual compressive strength of the concrete. Additionally, the maximum temperature reached by the steel components during the fire was considered, to determine their residual load-bearing capacity. The residual load-bearing capacity was estimated using Eqs 1 and 2. The residual strength of the steel was determined according to the work developed by Neves et al. [3], and the residual strength of concrete heated to a maximum temperature $\theta_{c,max}$ and cooled to an ambient temperature of 20 °C, was obtained according to Annex C of EN1994-1-2 [12]. The maximum temperatures in the steel rebars, in the collaborating steel deck, and in the unexposed surface of the composite slabs, were used to calculate the residual load-bearing capacity are presented in Table 3.

Table 3. Maximum temperature reached on the components with 100 mm concrete cover.

Profile geometry	Fire scenario	Rebar temp. (°C)	Web temp. (°C)	Lower flange temp. (°C)	Upper flange temp. (°C)	Unexposed surface temp. (°C)
Polideck 59S	Parametric 1	333.12	703.90	756.62	691.31	151.70
Bondeck	Parametric 2	360.00	746.80	872.70	606.90	176.00
Multideck 50	Parametric 3	569.60	917.80	994.10	816.70	286.00
Confraplus 60	Parametric 4	375.60	937.30	997.00	940.60	144.60

For sections with lower concrete cover thicknesses, such as the $h_1 = 40$ mm thickness models, the temperatures on the unexposed surface reach considerably higher values, which may have a big influence on the residual load-bearing capacity of these structural elements. However, the temperature variation along the unexposed surface is also notable, making it difficult to predict a single representative temperature value to consider the reduction of concrete load-bearing capacity. This is not the case with composite slabs with $h_1 = 100$ mm thickness. Figure 20 presents the coefficients to determine the load-bearing capacity of concrete and steel at room temperature, after being submitted to the maximum temperature reached during the fire.

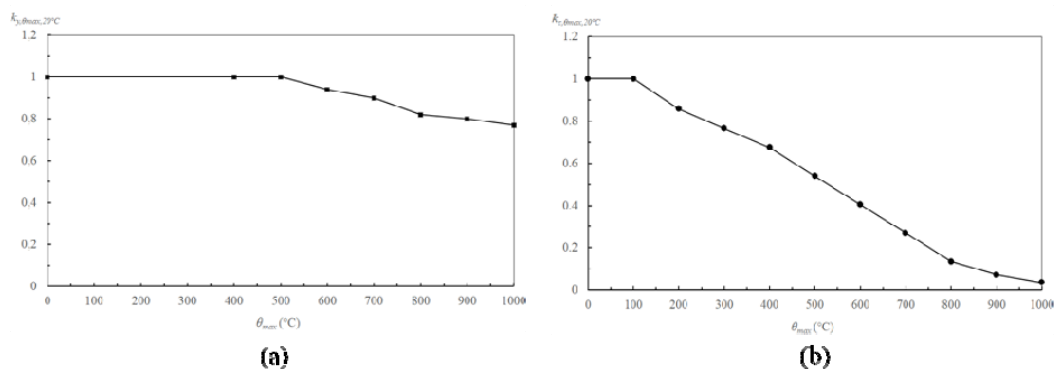


Figure 20. Coefficients to determine residual strength after cooling. (a) Residual strength of steel after cooling [3]; (b) Residual strength of concrete after cooling [12].

Table 4 presents the results of the load-bearing capacity of the composite slabs at room temperature before fire exposure, the residual load-bearing capacity after a fire, when all the components of the slab have reached room temperature, and the corresponding loss of load-bearing capacity.

Table 4. The residual load-bearing capacity of the composite slabs.

Profile geometry	Fire scenario	Load-bearing capacity (kN/m ²)	Residual load-bearing capacity (kN/m ²)	Loss of load-bearing capacity (%)
Polideck 59S	Parametric 1	31.25	28.31	09.40
Bondeck	Parametric 2	40.66	34.59	14.94
Multideck 50	Parametric 3	50.02	42.25	20.31
Confraplus 60	Parametric 4	38.63	31.99	17.18

For the first three composite slabs, which were subjected to fire curves with the same heating rate but different heating phase periods, it can be seen that the higher the time and maximum temperature of the gas in the heating stage, the higher is the loss of load-bearing capacity. This is expected as such factors indicate a higher temperature reached in the steel components as well as in the compressed region of the concrete. Moreover, the composite slab with Confraplus 60 steel deck profile highlights the influence of the residual strength of the steel components in determining the residual load-bearing capacity of composite slabs, as it was subjected to the Parametric 4 fire scenario. This profile obtained higher temperatures in the steel components, which are closer to the heat source, and lower temperatures on the unexposed surface. It can also be seen that the Confraplus 60 profile, subjected to Parametric 4 fire scenario, shows a higher loss of load-bearing capacity when compared to the Bondeck profile, subjected to Parametric 2 fire scenario. Although the Bondeck profile is subjected to a heating phase twice as long as the Confraplus 60 profile, the maximum temperature dictated the amount of the loss of the load-bearing resistance. On the other hand, the Confraplus 60 profile, subjected to Parametric curve 4, presents a loss of load-bearing capacity smaller than the Multideck 50 profile, subjected to the Parametric 3 fire scenario. In this case, although the maximum temperatures of the gas and steel components have close values, the long heating phase of Parametric curve 3 causes sufficient time to raise the temperature on the unexposed surface of the slab, reaching much higher values in the Multideck 50 profile, consequently resulting in a higher loss of compressive strength of the concrete and the slab resistant capacity.

4. Conclusions

The three-dimensional numerical model was developed in MATLAB and ANSYS programs and validated based on experimental results. The models considered the detachment effect between the steel deck and the concrete, which occurs due to the difference in thermal expansion of the materials. This effect was modeled in MATLAB with solid finite elements, and in ANSYS with shell finite elements to increase the accuracy of the numerical results. A slight difference between the numerical and experimental results was found, and this difference can be attributed to the types and shapes of finite elements used, to the effect of the convective coefficient during the cooling stage, and the effects of temperature increase on the exposed surface of the slab, which causes moisture migration towards the unexposed face, causing changes in the thermal properties of concrete that

were not explicitly considered in the models.

A parametric study was developed to evaluate the behaviour of the neutral axis, the load-bearing capacity of the composite slabs during a fire, and the residual load-bearing capacity of the slabs, using the temperatures in the components. The temperatures of these components were used to determine the mechanical strength of the materials, which are responsible for the reduction in bending resistance. Results also demonstrated a possible reduction of 20% with respect to the original load-bearing resistance on composite slabs when submitted to long fire events (Parametric 3 fire scenario).

It was possible to see that the heating and cooling rates also directly influence the reduction and recovery rate of the load-bearing capacity of composite slabs. It should be noted that the composite slabs subjected to the same fire scenario, with the same geometric profile and different cover thickness h_1 , reached a similar minimum relative load-bearing capacity.

Furthermore, it was observed that the behaviour of the load-bearing capacity curve follows the behaviour of the neutral axis curve along with the fire and that the lowest load-bearing capacity occurs during the cooling phase. These results show the real risk of a natural fire in the safety of composite slabs with steel decks during the cooling phase.

It was also found that for fire scenarios with similar heating phase duration, the maximum gas temperature and the residual strength of the steel components will determine the magnitude of the loss of the load-bearing capacity of the slabs in the post-fire. On the contrary, for fire scenarios with similar maximum gas temperatures but distinct heating phase duration, the heating time and the residual compressive strength of concrete will determine the residual load-bearing capacity of the slabs.

Thus, this work demonstrates the importance of performing accurate thermal analyses and using reduction coefficients applied to the strength capacity of steel, to obtain the load-bearing resistance during the heating and cooling phase, as well as in determining the residual strength of the structural element. Moreover, although the Eurocode EN1994-1-2 neglects the temperature effect on concrete properties, it is important to note that the effects of the loss of load-bearing capacity of the concrete cannot be neglected, because, in some natural fire scenarios, it will be decisive to determine the residual load-bearing capacity, being important to investigate efficient ways to consider and apply such losses.

Conflict of interest

There is no conflict of interest between authors.

References

1. Jiang J, Main JA, Weigand JM, et al. (2018) Thermal performance of composite slabs with profiled steel decking exposed to fire effects. *Fire Safety J* 95: 25–41. <https://doi.org/10.1016/j.firesaf.2017.10.003>
2. Pantousa D, Mistakidis E (2013) Advanced modeling of composite slabs with thin-walled steel sheeting submitted to fire. *Fire Technol* 49: 293-327. <https://doi.org/10.1007/s10694-012-0265-x>

3. Neves IC, Rodrigues JPC, Loureiro ADP (1996) Mechanical properties of reinforcing and prestressing steels after heating. *J Mater Civil Eng* 8: 189–194. [https://doi.org/10.1061/\(ASCE\)0899-1561\(1996\)8:4\(189\)](https://doi.org/10.1061/(ASCE)0899-1561(1996)8:4(189))
4. Kodur V (2014) Properties of concrete at elevated temperatures. *ISRN Civ Eng* 2014: 468510. <https://doi.org/10.1155/2014/468510>
5. Chan YN, Peng GF, Anson M (1999) Residual strength and pore structure of high-strength concrete and normal strength concrete after exposure to high temperatures. *Cement Concrete Comp* 21: 23–27. [https://doi.org/10.1016/S0958-9465\(98\)00034-1](https://doi.org/10.1016/S0958-9465(98)00034-1)
6. Gillie M, Usmani A, Rotter M, et al. (2001) Modelling of heated composite floor slabs with reference to the Cardington experiments. *Fire Safety J* 36: 745–767. [https://doi.org/10.1016/S0379-7112\(01\)00038-8](https://doi.org/10.1016/S0379-7112(01)00038-8)
7. Li GQ, Zhang N, Jiang J (2017) Experimental investigation on thermal and mechanical behaviour of composite floors exposed to standard fire. *Fire Safety J* 89: 63–76. <https://doi.org/10.1016/j.firesaf.2017.02.009>
8. Filho MMA (2020) Influence of the cooling phase in the fire resistance of composite slabs with steel deck [Master's thesis]. Instituto Politécnico de Bragança/Instituto Federal Alagoas (In Portuguese). Available from: <http://hdl.handle.net/10198/23536>.
9. Nguyen MP, Nguyen TT, Tan KH (2018) Temperature profile and resistance of flat decking composite slabs in- and post-fire. *Fire Safety J* 98: 109–119. <https://doi.org/10.1016/j.firesaf.2018.04.001>
10. Nguyen MP, Nguyen TT, Tan KH (2017) Assessment of damage and residual load bearing capacity of a concrete slab after fire: Applied reliability-based methodology. *Eng Struct* 150: 969–985. <https://doi.org/10.1016/j.engstruct.2017.07.078>
11. CEN-European Committee for Standardization (2020) Fire resistance tests-Part 1: General requirements. EN 1363-1.
12. CEN-European Committee for Standardization (2005) Eurocode 4-Design of composite steel and concrete structures-Part 1-2: General rules-Structural fire design. EN 1994-1-2.
13. Jiang J, Pintar A, Weigand JM, et al. (2019) Improved calculation method for insulation-based fire resistance of composite slabs. *Fire Safety J* 105: 144–153. <https://doi.org/10.1016/j.firesaf.2019.02.013>
14. Bolina F, Tutikian B, Rodrigues JPC (2021) Thermal analysis of steel decking concrete slabs in case of fire. *Fire Safety J* 121: 103295. <https://doi.org/10.1016/j.firesaf.2021.103295>
15. Lamont S, Usmani AS, Drysdale DD (2001) Heat transfer analysis of the composite slab in the Cardington frame fire tests. *Fire Safety J* 36: 815–839. [https://doi.org/10.1016/S0379-7112\(01\)00041-8](https://doi.org/10.1016/S0379-7112(01)00041-8)
16. Guo S, Bailey CG (2011) Experimental behaviour of composite slabs during the heating and cooling fire stages. *Eng Struct* 33: 563–571. <https://doi.org/10.1016/j.engstruct.2010.11.014>
17. Guo S (2012) Experimental and numerical study on restrained composite slab during heating and cooling. *J Constr Steel Res* 69: 95–105. <https://doi.org/10.1016/j.jcsr.2011.08.009>
18. CEN-European Committee for Standardization (2009) Fire classification of construction products and building elements. EN 13501-2.
19. CEN-European Committee for Standardization (2014) Fire resistance tests for loadbearing elements-Part 2: Floors and roofs. EN 1365-2.

20. Both C (1998) The fire resistance of composite steel-concrete slabs [PhD's thesis]. Delft University Press.
21. Piloto PAG, Prates LMS, Balsa C, et al. (2018) Numerical simulation of the fire resistance of composite slabs with steel deck. *Int J Eng Technol* 7: 83–86. <https://doi.org/10.14419/ijet.v7i2.23.11889>
22. Piloto P, Prates L, Balsa C, et al. (2019) Fire resistance of composite slabs with steel deck: From Experiments to numerical simulation. *Mecânica Exp* 31: 85–94.
23. Piloto PAG, Balsa C, Ribeiro F, et al. (2021) Computational simulation of the thermal effects on composite slabs under fire conditions. *Math Comput Sci* 15: 155–171. <https://doi.org/10.1007/s11786-020-00466-0>
24. Piloto PAG, Balsa C, Santos LMC, et al. (2020) Effect of the load level on the resistance of composite slabs with steel decking under fire conditions. *J Fire Sci* 38: 212–231. <https://doi.org/10.1177/0734904119892210>
25. Jiang J, Cai W, Chen W, et al. (2021) An insight into eurocode 4 design rules for thermal behaviour of composite slabs. *Fire Safety J* 120: 03084. <https://doi.org/10.1016/j.firesaf.2020.103084>
26. CEN-European Committee for Standardization (2002) Eurocode 1: Actions on structures-Part 1-2: General actions-Actions on structures exposed to fire. EN 1991-1-2.
27. CEN-European Committee for Standardization (2005) Eurocode 3: Design of steel structures-Part 1-2: General rules-Structural fire design. EN 1993-1-2.
28. Çengel YA, Ghajar AJ (2015) *Heat and Mass Transfer: Fundamentals and Applications*, 5 Eds., New York: McGraw-Hill Education.
29. ISO (1999) Fire-resistance tests-Elements of building construction. ISO 834.
30. Tao Z, Wang XQ, Uy B (2013) Stress-strain curves of structural and reinforcing steels after exposure to elevated temperatures. *J Mater Civ Eng* 25: 1306–1316. [https://doi.org/10.1061/\(ASCE\)MT.1943-5533.0000676](https://doi.org/10.1061/(ASCE)MT.1943-5533.0000676)
31. Piloto PAG, Mesquita L, Real PV, et al. (2002) Steel mechanical properties evaluated at room temperature after being submitted at fire conditions. *XXX Iahs World Congress on Housing, Housing Construction: an Interdisciplinary Task*, 1–3.
32. Hamerlinck AF (1991) *The Behaviour of Fire-Exposed Composite Steel/Concrete Slabs*, Eindhoven University of Technology.
33. Gernay T, Franssen J (2015) A performance indicator for structures under natural fire. *Eng Struct* 100: 94–103. <https://doi.org/10.1016/j.engstruct.2015.06.005>



AIMS Press

© 2022 the Author(s), licensee AIMS Press. This is an open access article distributed under the terms of the Creative Commons Attribution License (<http://creativecommons.org/licenses/by/4.0>)